EPJ Web of Conferences **302**, 07002 (2024) https://doi.org/10.1051/epjconf/202430207002
SNA + MC 2024

Neutron resonance cross sections evaluation based on the phase shift deep neural network

Zehua Hu*

Institute of Applied Physics and Computational Mathematics, 100094, Beijing, China

Abstract. Neutron resonance cross sections are essential in many nuclear science and application fields. Evaluated nuclear libraries usually derive neutron resonance parameters using R-matrix theory. However, determining these parameters and reconstructing the pointwise cross sections required for transport calculations is a time-consuming process. This paper presents a new method for fitting neutron resonance cross sections by using a phase shift deep neural network (PhaseDNN). The network presents resonance cross sections based on its network parameters. This approach allows for the quick calculation of cross section values from the given network parameters. Additionally, PhaseDNN can fit network parameters to experimental data to obtain a smooth resonance cross section curve. Therefore, it has the potential to be an alternative to R-matrix theory.

1 Introduction

Accurate nuclear reaction data, particularly neutron data, are essential for scientific and engineering advances in many fields[1–4], including nuclear energy, national security, and nuclear medicine. Cross sections are nuclear data that describe the probability that an incident particle will react with the target nucleus. These are primarily derived from nuclear physics experiments[5].

In the resonance energy region, neutron cross sections for elastic scattering, fission, and radiative capture of heavy isotopes exhibit significant fluctuations with incident neutron energy, with peaks at specific energies. Resonance cross sections are typically described by various approximate R-matrix theory formulae[6]. The parameters of these formulae are determined by examining experimental data and then stored in the evaluation nuclear libraries.

In recent years, machine learning techniques have been increasingly used for nuclear data evaluation. Vicente-Valdez et al[7] applied the random forest and K-nearest neighbour methods to evaluate the cross sections of ^{233}U and ^{35}Cl. However, both methods showed significant over-fitting, leading the authors to recommend the use of the more powerful deep neural network (DNN) method for resonance evaluation.

* Corresponding author:hu_zehua@iapcm.ac.cn

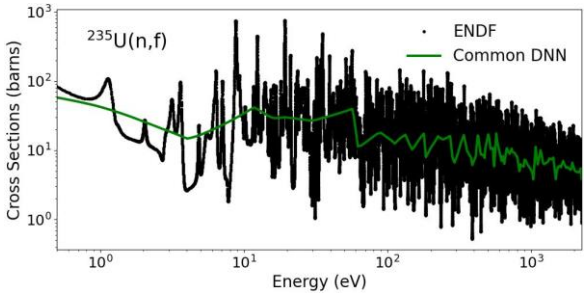

Fig. 1. Cross sections of ^{235}U(n,f) fitted using a common deep neural network (DNN) with an structure of 1-200-200-200-800-1 (one neuron in the input layer, 200 neurons in each of the three hidden layers, 800 neurons in the last hidden layers, and one neuron in the output layer). The reconstructed ^{235}U(n,f) cross sections from ENDF/B-VIII.0 are represented by the black dot (ENDF), while the green line shows the corresponding result obtained using the common DNN.

In order to test the ability of the deep neural network to approximate the resonance cross sections of heavy isotopes, we reconstructed the resonance parameters of ^{235}U from the ENDF/B-VIII.0 library[8] into pointwise cross sections using NJOY[9]. These point-wise cross sections are referred to as PENDF data. We utilised the PENDF resonance cross sections as the dataset to train a fully connected deep neural network and predict the resonance cross sections. The results are presented in Figure 1. The limitations of the common neural network are evident in its inability to fit the fluctuations of the resonance cross sections of ^{235}U. The question that arises is how to fit resonance cross sections based on deep neural networks.

2 Phase shift deep neural network

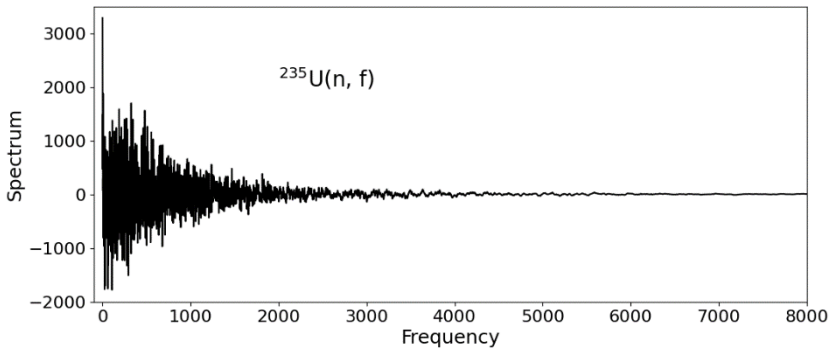

Fig. 2. Frequency spectrum of ^{235}U resonance cross-section. Frequency spectrum obtained by Fourier transform, showing
very broad spectrum.

Study[10] shown that during training, DNNs tend to fit target functions from low to high frequency components, which is known as the frequency principle (F-principle). The resonance cross sections can be converted from the time domain to the frequency domain by means of the Fourier transform. The frequency spectrum of the cross sections is obtained through the application of the fast Fourier transform. Figure 2 shows a super wide frequency range, with high frequencies reaching 4000-6000. Fully connected deep neural networks are only capable of fitting the low-frequency components of the resonance cross sections. Only

the mean values of the resonance cross sections corresponding to the low-frequency components are provided, as shown in Figure 1.

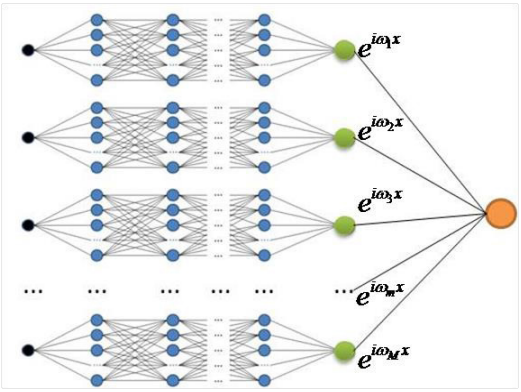

Fig. 3. Coupled phase shift deep neural network (PhaseDNN). PhaseDNN consists of a series of DNNs as sub-networks; each DNN is responsible for processing a specific high frequency band in conjunction with a phase shift factor e^{-iwmx}. The results of the sub-networks are then summed to approximate the target function.

Cai et al. proposed a phase shift deep neural network (PhaseDNN)[11] that follows the frequency principle. PhaseDNN provides uniform broadband convergence when approximating high-frequency functions. In the frequency domain, the frequency is divided into a series of smaller frequency intervals. Then, a series of medium-sized DNNs are constructed and trained for each of the frequency intervals with a phase shift factor. PhaseDNN can convert high-frequency learning into low-frequency learning to achieve unified learning for broadband function.

Figure 3 displays a coupled PhaseDNN[11] that is utilized to fit a wideband function. The frequency grid is defined as $\{\omega_m\}_{m=1}^{M}$, with a frequency increment of $\Delta\omega = \omega_m - \omega_{m-1}$. The function in time domain for each frequency band m is represented by $f_m(x)$, and the function representing the shifted lowest frequency corresponding to band m is denoted as $s_m(x)$,

$$f_m(x) = s_m(x)e^{-i\omega_m x}$$

The output of each sub-network in the coupled network simulates a phase-shifted function $s_m(x)$ for a specific frequency band. This function is low frequency and can be easily fitted according to the frequency principle, making the coupled PhaseDNN easy to train.

3 Approximation of resonance cross sections using PhaseDNN

The coupled PhaseDNN model is used to approximate ^{235}U neutron fission cross sections from the evaluated library ENDF[12] and the experimental library EXFOR[5] libraries.

3.1 Evaluated cross sections

The ENDF data, derived from a combination of experimental data and theoretical calculations, can be considered as clean data. The ENDF/B-VIII.0 library[8] provides the resonance cross sections of ^{235}U for fission, elastic scattering, and radiative capture in terms of 3195 resonances in the Resolved Resonance Range. Each resonance contains 6 resonance parameters, resulting in a total of 19170 parameters. The point-wise cross sections (PENDF) of ^{235}U fission are prepared from the resonance parameters using the NJOY code[9] with a

reconstruction tolerance of 0.001 and a reconstruction temperature of 293.6K and used as training data. The training data are given as a table of about 76000 energy-cross section pairs, with linear interpolation, and energy grid is directly sourced from NJOY.

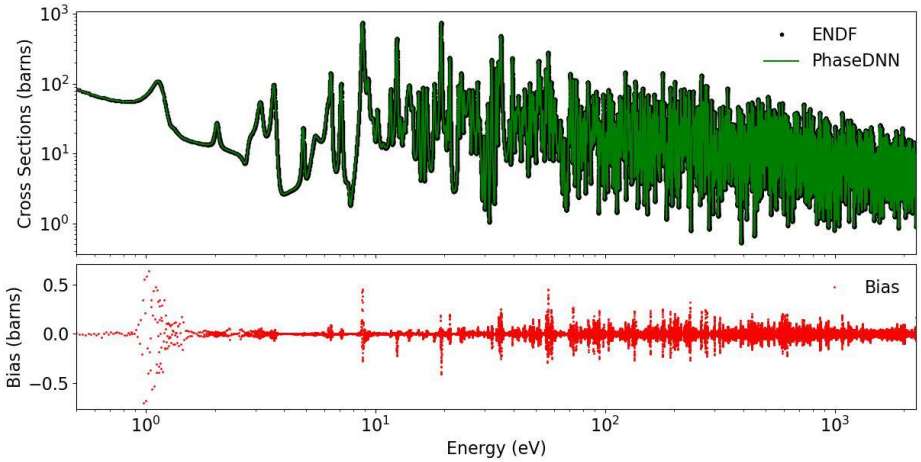

Fig. 4. The fitting result for the cross sections of ^{235}U fission from ENDF using the PhaseDNN. The upper plot compares the cross sections reconstructed by NJOY from ENDF evaluation with those predicted by PhaseDNN, while the lower plot shows the difference between them.

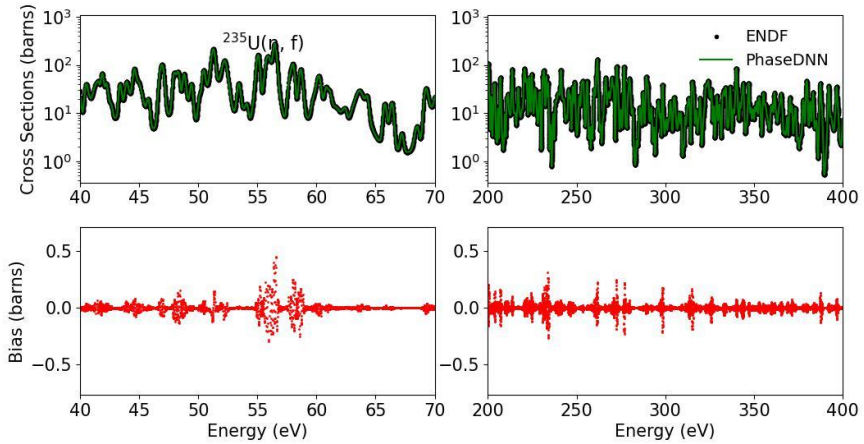

Fig. 5. The detail fitting result for the cross sections of ^{235}U fission from ENDF using the PhaseDNN.

The frequency number is truncated to 4000, and the frequency increment $\Delta\omega$ is set to 10, resulting in 400 frequency bands. To learn the real and imaginary parts of each band, two DNNs are constructed. Therefore, 800 DNNs are required in the coupled PhaseDNN. Each DNN consists of 3 hidden layers, with 40 neurons in each layer. Thus, the DNN structure is 1-40-40-40-1. The PhaseDNN was trained for 20000 epochs using the Adam optimizer with a learning rate of 1e-4. Figure 4 displays the training results. The coupled PhaseDNN effectively captures all resonances in the ^{235}U fission cross sections and approximates the cross sections accurately. Further details are presented in Figure 5. The PhaseDNN provides

an accurate approximation of the complex resonance cross sections, with only slightly larger deviations observed near the resonance peaks.

3.2 Experimental cross sections

Main motivation of this study is data evaluation, i.e. the derivation of complete, self-consistent energy-cross section curves from experimental data. As seen above, PhaseDNN accurately reproduces the complex ^{235}U fission cross sections from the ENDF library. Therefore, it is reasonable to expect that this network could be utilised to evaluate experimental resonance data.

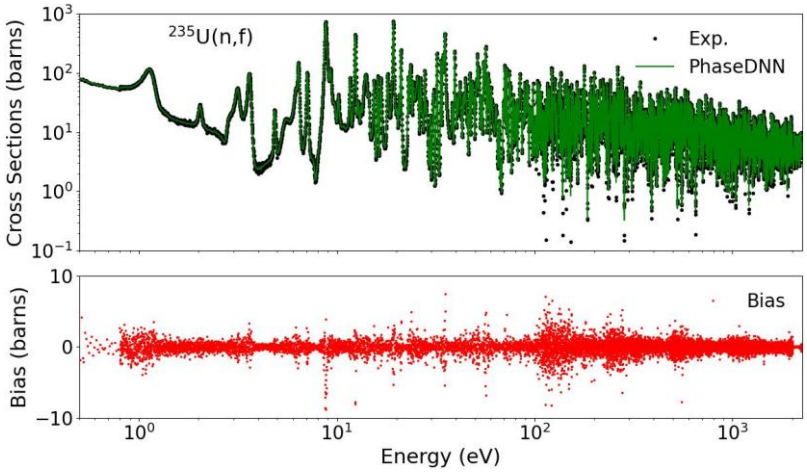

Fig. 6. The fitting result for the cross sections of ^{235}U fission from EXFOR using the PhaseDNN. The upper plot compares the cross sections from EXFOR with those predicted by PhaseDNN, while the lower plot shows the difference between them.

To minimize the risk of overfitting caused by noise in the experimental cross sections, the number of neurons in the hidden layer is reduced to 20, and the number of frequency bands is decreased to 200. The DNN structure is set to 1-20-20-20-1, and 400 DNNs are used. The results are presented in Figure 6, which shows that the coupled PhaseDNN approximates the experimental cross sections of ^{235}U reasonably well. Detailed results are shown in Figure 7.

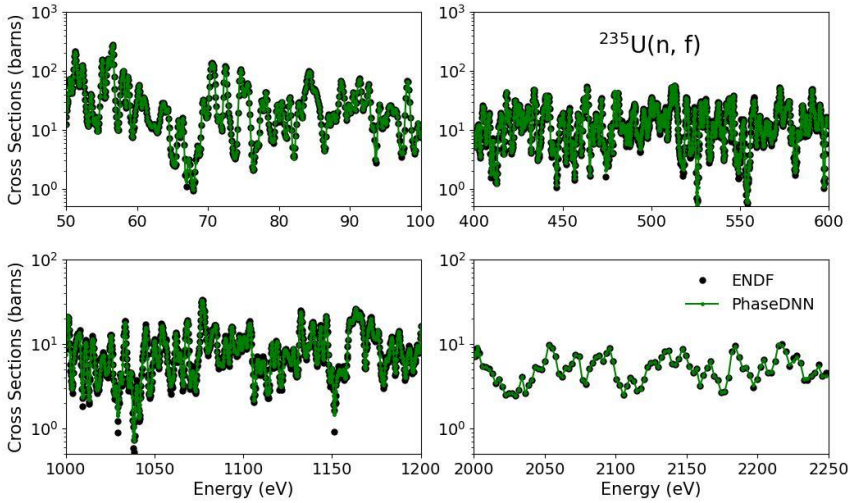

Fig. 7. The detail fitting result for the cross sections of ^{235}U fission from EXFOR using the PhaseDNN.

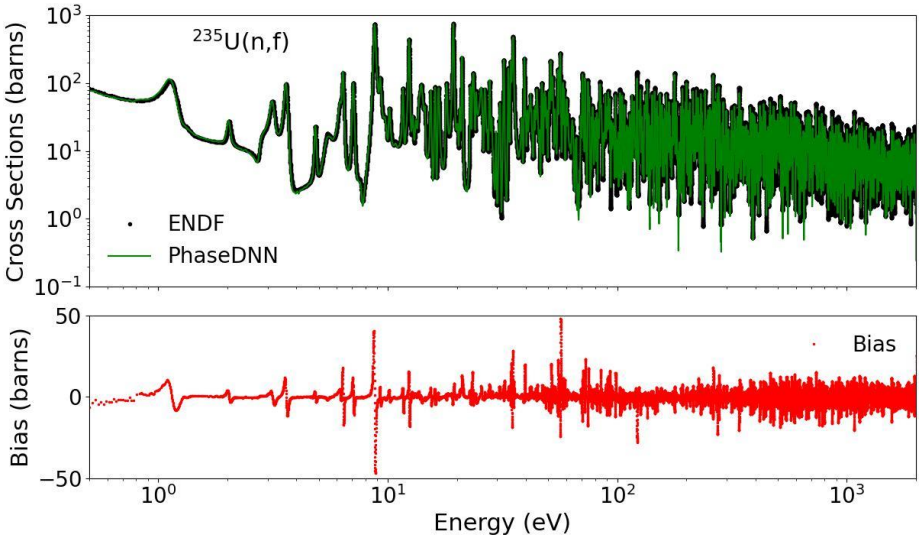

Fig. 8. Prediction on ENDF point-wise energy points. The upper plot shows the PENDF data from ENDF/B-VIII.0 as black dots, and the green line represents the prediction of the coupled PhaseDNN on the PENDF energy grid. The lower plot displays the difference between the prediction and PENDF data.

The PhaseDNN model, trained using experimental data, predicts resonance cross sections on the PENDF energy grid. Figure 8 displays the predicted results, which are in good agreement with the evaluated data from ENDF/B-VIII.0. The deviation is roughly within the uncertainty range of the experimental data.

4 Summary

The coupled PhaseDNN is used to fit heavy isotope resonance cross sections in the ENDF and EXFOR libraries. The ENDF data can be fit very accurately. The experimental cross sections can also be fitted reasonably well with a smaller PhaseDNN, and the network trained on experimental data predicts satisfactory results. With further refinement, PhaseDNN is expected to become a new method for resonance cross section evaluation.

References

(1) Forrest, R. A. Nuclear Science and Data Needs for Advanced Nuclear Systems. *Energy Procedia* **2011**, *7*, 540–552. https://doi.org/10.1016/j.egypro.2011.06.075.
(2) Bernstein, L. A.; Brown, D.; Hurst, A. M.; Kelley, J. H.; Kondev, F. G.; McCutchan, E. A.; Nesaraja, C. D.; Slaybaugh, R.; Sonzogni, A. *Nuclear Data Needs and Capabilities for Applications Whitepaper*; LLNL-CONF-676585; Lawrence Livermore National Lab. (LLNL), Livermore, CA (United States), 2015. https://www.osti.gov/biblio/1229857 (accessed 2024-02-24).
(3) Bernstein, L. A.; Brown, D. A.; Koning, A. J.; Rearden, B. T.; Romano, C. E.; Sonzogni, A. A.; Voyles, A. S.; Younes, W. Our Future Nuclear Data Needs. *Annu. Rev. Nucl. Part. Sci.* **2019**, *69* (1), 109–136. https://doi.org/10.1146/annurev-nucl-101918-023708.
(4) Kolos, K.; Sobes, V.; Vogt, R.; Romano, C. E.; Smith, M. S.; Bernstein, L. A.; Brown, D. A.; Burkey, M. T.; Danon, Y.; Elsawi, M. A.; Goldblum, B. L.; Heilbronn, L. H.; Hogle, S. L.; Hutchinson, J.; Loer, B.; McCutchan, E. A.; Mumpower, M. R.; O'Brien, E. M.; Percher, C.; Peplowski, P. N.; Ressler, J. J.; Schunck, N.; Thompson, N. W.; Voyles, A. S.; Wieselquist, W.; Zerkle, M. Current Nuclear Data Needs for Applications. *Phys. Rev. Res.* **2022**, *4* (2), 021001. https://doi.org/10.1103/PhysRevResearch.4.021001.
(5) Zerkin, V. V.; Pritychenko, B. The Experimental Nuclear Reaction Data (EXFOR): Extended Computer Database and Web Retrieval System. *Nucl. Instrum. Methods Phys. Res. Sect. Accel. Spectrometers Detect. Assoc. Equip.* **2018**, *888*, 31–43. https://doi.org/10.1016/j.nima.2018.01.045.
(6) *Rev. Mod. Phys. 30, 257 (1958) - R-Matrix Theory of Nuclear Reactions*. https://journals.aps.org/rmp/abstract/10.1103/RevModPhys.30.257 (accessed 2024-01-26).
(7) Vicente-Valdez, P.; Bernstein, L.; Fratoni, M. Nuclear Data Evaluation Augmented by Machine Learning. *Ann. Nucl. Energy* **2021**, *163*, 108596. https://doi.org/10.1016/j.anucene.2021.108596.
(8) Brown, D. A.; Chadwick, M. B.; Capote, R.; Kahler, A. C.; Trkov, A.; Herman, M. W.; Sonzogni, A. A.; Danon, Y.; Carlson, A. D.; Dunn, M.; Smith, D. L.; Hale, G. M.; Arbanas, G.; Arcilla, R.; Bates, C. R.; Beck, B.; Becker, B.; Brown, F.; Casperson, R. J.; Conlin, J.; Cullen, D. E.; Descalle, M.-A.; Firestone, R.; Gaines, T.; Guber, K. H.; Hawari, A. I.; Holmes, J.; Johnson, T. D.; Kawano, T.; Kiedrowski, B. C.; Koning, A. J.; Kopecky, S.; Leal, L.; Lestone, J. P.; Lubitz, C.; Márquez Damián, J. I.; Mattoon, C. M.; McCutchan, E. A.; Mughabghab, S.; Navratil, P.; Neudecker, D.; Nobre, G. P. A.; Noguere, G.; Paris, M.; Pigni, M. T.; Plompen, A. J.; Pritychenko, B.; Pronyaev, V. G.; Roubtsov, D.; Rochman, D.; Romano, P.; Schillebeeckx, P.; Simakov, S.; Sin, M.; Sirakov, I.; Sleaford, B.; Sobes, V.; Soukhovitskii, E. S.; Stetcu, I.; Talou, P.; Thompson, I.; van der Marck, S.; Welser-Sherrill, L.; Wiarda, D.; White, M.; Wormald, J. L.; Wright, R. Q.; Zerkle, M.; Žerovnik, G.; Zhu, Y. ENDF/B-VIII.0: The 8th Major Release of the Nuclear Reaction Data Library with CIELO-Project Cross Sections, New Standards and Thermal Scattering Data. *Nucl. Data Sheets* **2018**, *148*, 1–142. https://doi.org/10.1016/j.nds.2018.02.001.

(9) R. E. MacFarlane; D. W. Muir; R. M Boicourt; A. C. Kahler; J. L. Conlin; W. Haeck. *The NJOY Nuclear Data Processing System, Version 2016*; LA-UR-17-20093; Los Alamos National Laboratory.
(10) *Frequency Principle: Fourier Analysis Sheds Light on Deep Neural Networks | Request PDF*. https://www.researchgate.net/publication/347008151_Frequency_Principle_Fourier_Analysis_Sheds_Light_on_Deep_Neural_Networks (accessed 2024-03-18).
(11) Cai, W.; Li, X.; Liu, L. A Phase Shift Deep Neural Network for High Frequency Approximation and Wave Problems. *SIAM J. Sci. Comput.* **2020**, *42* (5), A3285–A3312. https://doi.org/10.1137/19M1310050.
(12) A. Trkov; M. Herman; D. A. Brown; N. Holden; G. Hedstrom. *ENDF-6 Formats Manual, Data Formats and Procedures for the Evaluated Nuclear Data Files ENDF/B-VI, ENDF/B-VII and ENDF/B-VIII*; BNL-203218-2018-INRE; National Nuclear Data Center, Brookhaven National Laboratory, 2018.